Check for updates

Source apportionment and ecological and health risk mapping of soil heavy metals based on PMF, SOM, and GIS methods in Hulan River Watershed, Northeastern China

**Yiming Xu · Xianxia Wang · Guannan Cui ·
Ke Li · Yanfeng Liu · Bin Li · Zhiliang Yao**

Abstract Heavy metals in agricultural soils not only affect the food security and soil security, but also endanger the human health through the food chain. Based on the incorporation of index analysis, positive matrix factorization (PMF), self-organizing map (SOM), and geostatistical methods, this research performed the assessment of source apportionment and ecological and health risks of soil heavy metals in Hulan River Watershed, Northeastern China. According to the Pollution Load Index (PLI), 83.08% of the soil samples were slightly or mildly polluted, and 1.54% of the soil samples were severely polluted. The ecological risk index (EI) showed that about 80.77%
and 60.77% of the soil samples were beyond the low risk level for Hg and Cd, respectively. In this research, the non-carcinogenic and carcinogenic risk indices for children were higher than adult males and adult females. Four potential sources were revealed based on the PMF and SOM analysis including atmospheric deposition and industrial emission; transportation source; agricultural source; and a combination of agricultural, industrial, and natural sources. Considerable and high ecological risk from Hg existed in the area close to the coal steam-electric plant, and considerable and high ecological risk from Cd existed in the Hulan River estuary area. The eastern part of the study area experienced higher non-carcinogenic and carcinogenic risks for adults and children than the western part of the study area. The source apportionment and ecological and health risk mapping provide important role in reducing pollution sources. Zonal pollution control and soil restoration measures should be performed in the areas with high ecological and health risks.

Y. Xu · X. Wang · G. Cui · K. Li · Y. Liu · B. Li ·
Z. Yao (✉)
School of Ecology and Environment, Beijing Technology and Business University, Beijing 100048, China
e-mail: yaozhl@th.btbu.edu.cn

Y. Xu · G. Cui · K. Li · Z. Yao
State Environmental Protection Key Laboratory of Food Chain Pollution Control, Beijing Technology and Business University, Beijing 100048, China

Y. Xu · G. Cui · K. Li · Z. Yao
Key Laboratory of Cleaner Production and Integrated Resource Utilization of China National Light Industry, Beijing Technology and Business University, Beijing 100048, China

Introduction

Soil heavy metal pollution severely threatens agro-ecosystem stability and food security. Different from

organic matter, most heavy metals are prone to transform to more toxic methyl compounds and do not degrade naturally. Heavy metals in agricultural soils can not only affect the soil security, grain output, and quality, but also endanger the health of human body through the food chain (Hou et al., 2020). Some research indicated that excessive exposure to the heavy metals could cause body damages and increase the cancer risks (Setia et al., 2021; Wang et al., 2020a, b, c, d). Long term accumulation of soil heavy metals can bring about the soil nutrient loss and degradation of soil quality and soil function (Semenkov & Koroleva, 2020). Furthermore, soil heavy metals can cause secondary pollution by transferring to water (Karaouzas et al., 2021) and atmosphere (Wan et al., 2016). As a result, it is important to identify and map the source, ecological risks, and human health risks of soil heavy metals.

To analyze the effects of heavy metals on ecological environment and human health, multiple indices were proposed for heavy metal pollution assessment. Some indices including index of geoaccumulation (Muller, 1969), the enrichment factor (Buat-Menard & Chesselet, 1979), the contamination factor (Hakanson, 1980), and individual contamination factor (Ikem et al., 2003) were utilized to evaluate the individual soil heavy metal pollution. Some indices including Pollution Load Index (Wang et al., 2020a, b, c, d) were utilized to assess the multi-element heavy metal pollution status. Other indices including Ecological Risk Index (Hakanson, 1980; Zeng et al., 2020) and total cancer risk (Wu et al., 2020a, b) have been applied to evaluate the effects of heavy metals on environment and human health.

The sources of heavy metals in agricultural soils are either related to the anthropogenic activities or natural process. Intensive input from human activities including fertilizers, agrochemicals, wastewater irrigation, and automobile exhaust emissions is the major driving forces of heavy metal accumulation in agricultural soils (Fei et al., 2019). Apportioning the corresponding contributions of soil heavy metals is of great importance to implement effective source reduction and site-specific sustainable soil management measurements. The techniques which can identify and quantify the sources of heavy metals in soils can be classified into source identification and source quantification methods. Source identification methods, which aim to define the types of pollution sources, include principal component analysis (Yang et al., 2020) and cluster analysis (Pandey et al., 2014). Source quantification methods, which aim to perform the quantitative analysis of contributions from different sources, include chemical mass balance (CMB) (Shi et al., 2019) and positive matrix factorization (PMF) (Wu et al., 2020a, b). Among multiple receptor models, PMF method is an effective and widely used method for soil heavy metal apportionment. It does not require the prior knowledge of source profiles, and it is appropriate to be applied in areas with similar parent materials and agricultural management practices (Lv, 2019). By integrating PMF and self-organizing map (SOM), Bhuiyan et al. (2021) identified four sources of soil heavy metals in Dhaka district in Bangladesh. Christensen et al. (2018) analyzed the anthropogenic and geogenic sources of heavy metals in moss and natural surface soils in Norway by PMF and Principal Component Analysis (PCA) methods. The source contributions of heavy metals are affected by various factors including climate, hydrology, and topography. Most research just analyzed the concentrations of source contribution, while ignoring the associated health and ecological risks. As a result, this research combined source apportionment methods and ecological and human health risk assessment to quantify and map the sources and ecological and health risks of soil heavy metals.

Although receptor models can help identify the potential sources of heavy metal and explain the relationships between different soil heavy metals, they cannot explain the spatial correlations of soil heavy metals. Characterizing the spatial pattern of soil heavy metals can help identify and demarcate the areas with relatively high heavy metal concentration. Generally, geostatistical and data mining methods are two major methods that are used to characterize the spatial pattern of soil heavy metals. Random forest and land use regression model had been utilized to predict the spatial pattern of soil heavy metals in Dongli District, Tianjin (Wang et al. 2020a, b, c, d). Geostatistical methods such as ordinary kriging and Inverse Distance Weight (IDW) methods had been used to analyze the spatial correlations of soil heavy metals (Gujre et al., 2021; Sergeev et al., 2019). Geostatistical methods can also reveal the spatial structure and spatial variability of factors derived from receptor models. However, most of the research just analyzed the spatial pattern of soil heavy metals and did not explore the spatial pattern of source apportionment

factors, health risks, and ecological risks (Kharazi et al., 2021; Liu et al., 2021a, b; Sergeev et al., 2019). Most research could not provide site-specific recommendations to the reginal ecological security and food security management.

Songnen Plain, an important part of the northern Songliao Plain, is an important commodity grain base in China. To feed the growing population, multiple natural lands were converted to cropland in the Songnen Plain in the past decades (Mao et al., 2019). In addition, the increasing use of chemical fertilizer and excessive reclamation have also led to soil degradation and soil nutrient loss (Song et al., 2018). However, few research has performed the source apportionment, ecological risk assessment, and health risk assessment of soil heavy metals in this area before. The primary goals of this study were to (1) determine the concentration of soil heavy metals; (2) assess the source apportionment, ecological risk, and health risk of soil heavy metals; (3) map the spatial pattern of soil heavy metals and related source apportionment factors, ecological risks, and healthy risks; and (4) make recommendations to the soil and agricultural management in Hulan River Watershed in Harbin, Heilongjiang province, China.

Materials and methods

Study area description

Hulan River is a tributary of Songhua River located in the central part of Heilongjiang province, China. It origins from Xiao Hinggan Mountains, and then flows into the Songhua River in Hulan District of Harbin City, capital of Heilongjiang province. Hulan River Watershed in Harbin City experienced the northern temperate continental monsoon climate with a warm summer and a cold winter. The frozen period is from late October to late April in this area. The average temperature in July and January is 20–23 °C and $-21--26$ °C, respectively. The average annual precipitation is 574.7 mm. The soil type in Hulan River Watershed is *Moollisols* according to the USDA Taxonomy. Maize (*Zea mays. L.*) was the main cropping system in the region. In recent years, more and more corn fields are transformed to soybean field due to the high economic value and market demand of the soybean in China.

Soil sampling and analysis

The top soils (20 cm depth from the surface) of 144 soil samples were collected across the study area (Fig. 1). Each soil sample was a composite of 3 subsamples acquired from a 10 m × 10 m grid of land. All samples were dried at 25 °C for 2 weeks, and then grounded under 100 mesh, and passed through a 2-mm sieve. Approximately 0.25 g of soil sample was digested with concentrated HNO_3-HF-$HClO_4$ on an electric hot plate (Dang et al., 2021; Wu et al., 2019). The contents of soil Cd, Cr, Cu, Pb, Ni, and Zn were determined by inductively coupled plasma-mass spectrometry (ICP-MS) in Geological Bureau of Hunan province. The contents of heavy metals including As and Hg were determined by atomic fluorescence spectrometry (AFC) in Geological Bureau of Hunan province.

Assessment of soil heavy metal pollution

Pollution assessment of soil heavy metal

Single factor pollution index (PI) and Pollution Load Index (PLI) were applied to calculate the pollution level from each heavy metal and all heavy metals, respectively (Zang et al., 2017). PI and PLI were estimated as Eqs. (1) and (2), respectively,

$$PI = \frac{C_i}{B_i} \tag{1}$$

$$PLI = \sqrt[i]{PI_1 \times PI_2 \times PI_3 \times \ldots \cdots \times PI_i} \tag{2}$$

where C_i the concentration of the ith heavy metal in soil, and B_i is its geochemical baseline concentration in the study area (Sun et al., 2013). PI_i is the single factor PI of ith heavy metal in soil (Jiang et al., 2021). The categories of PI and PLI are shown in Table S1.

Potential ecological risk assessment of heavy metal pollution

Ecological risk index (EI) and Comprehensive ecological risk assessment (RI) can reflect the ecological impacts of a single heavy metal and all the soil heavy metals, respectively (Hakanson, 1980). The formula of EI and RI was calculated as follows:

Fig. 1 Soil sampling sites in Hulan River Watershed, Harbin, China
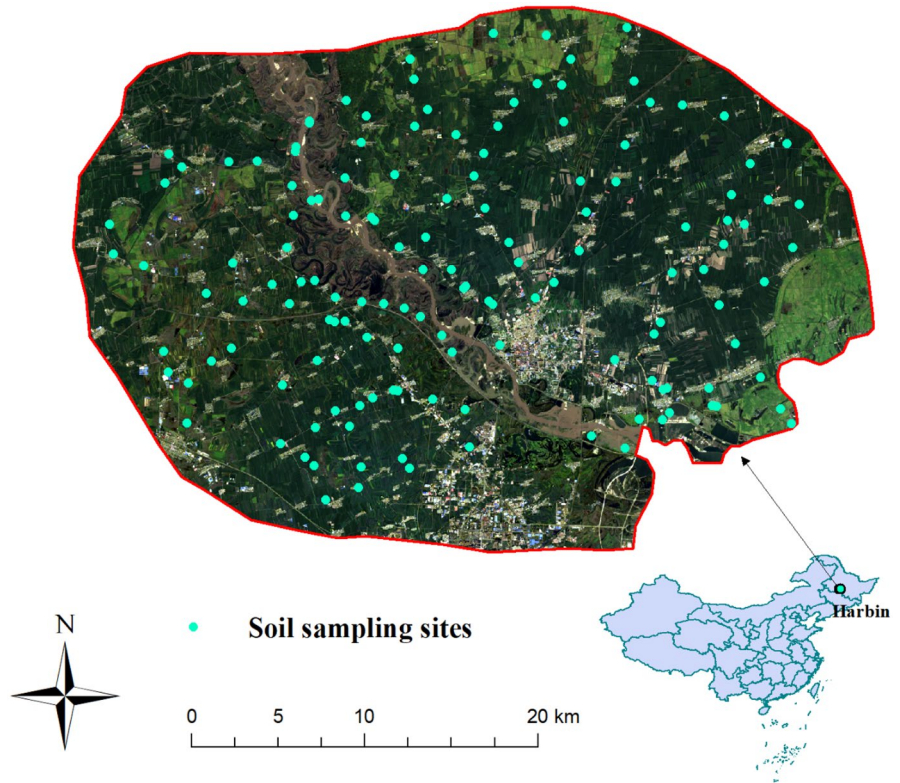
$$EI_i = T_i \times PI_i \tag{3}$$

$$RI = \sum_{i=1}^{n} EI_i \tag{4}$$

where T_i is the toxic-response factor (Zeng et al., 2020). The categories of RI and EI are also shown in Table S2.

Potential health risk evaluation of soil heavy metal

The human exposure risks from soil heavy metals were estimated by three different pathways including ingestion (ing), inhalation (inh), and dermal contact (der) (Zhao et al., 2019). In this study, the average daily intake (ADI) (mg/kg/day) of soil heavy metals for anthropic health risks through the following three pathways was estimated with Eqs. (5)–(7):

$$ADI_{ing} = \frac{C \times R_{ing} \times EF \times ED \times CF}{BW \times AT} \tag{5}$$

$$ADI_{inh} = \frac{C \times R_{ink} \times EF \times ED}{PEF \times BW \times AT} \tag{6}$$

$$ADI_{der} = \frac{C \times SA \times AF \times ABS \times EF \times ED \times CF}{BW \times AT} \tag{7}$$

The definition and values of exposure parameters are summarized in Table S3.

The total non-carcinogenic risk (THI) and total cancer risk (TCR) (Wu et al., 2020a, b) were calculated with Eqs. (8) and (9).

$$THI = \sum_{i=0}^{n} \frac{ADI_i}{RfD_i} \tag{8}$$

$$TCR = \sum_{i=0}^{n} ADI_i \times SF_i \tag{9}$$

where n is the number of soil heavy metals, ADI_i is the average daily intake for the ith soil heavy metal, RfD_i is the reference dose for the ith soil heavy metal, and SF_i is the slope factor for the ith soil heavy metal. If the THI value is higher than 1, there are potential non-carcinogenic effects. If the THI value is lower than 1, there is no risk of adverse health effect. If the TCR value is higher than $1E-04$, the cancer risk is unacceptable. If the TCR value is lower than $1E-04$, an acceptable risk for cancer can be expected (Wu et al., 2020a, b).

Statistical analysis

The descriptive analysis of the data was carried out in R software. The spatial distribution of heavy metals was characterized by Inverse Distance Weighted (IDW) method in ArcGIS 10.4.1. The factor scores from PMF analysis, PI, PLI, EI, RI, THI, and TCR were interpolated by IDW to show the pollution status and ecological and health risks in the study area.

PMF analysis

PMF (version 5.0) is a multivariate receptor model developed by Paatero and Tapper (1994). It was widely utilized to identify and quantify the sources of heavy metals in soil, sediments, and air (Brown et al., 2015; Christensen et al., 2018; Wu et al., 2020a, b). The calculation principle and expression of PMF are described as follows:

$$X_{ij} = \sum_{k=1}^{p} g_{ik}f_{kj} + e_{ij} \qquad (10)$$

where i is the soil sample number, j is the heavy metal category, p is the number of potential sources, X_{ij} is the sample data matrix, g_{ik} is the source contribution matrix, f_{kj} is the source profile matrix, and e_{ij} is the residual for each soil sample.

The purpose of the PMF is to achieve the minimum value of the objective function (Q(E)). The Q(E) is defined as:

$$Q(E) = \sum_{i=1}^{n} \sum_{j=1}^{m} \left(\frac{e_{ij}}{u_{ij}}\right)^2 \qquad (11)$$

where u_{ij} is the uncertainty. u_{ij} is calculated as the following formula:

$$u_{ij} = \begin{cases} \frac{5}{6} \times MDL, (c \leq MDL) \\ \sqrt{(\sigma \times c)^2 + (0.5 \times MDL)^2}, \ (c > MDL) \end{cases} \qquad (12)$$

where c is the soil heavy metal concentration, MDL is the method detection limit, and σ is a percentage of the measurement uncertainty.

Self-organizing map (SOM) analysis

A self-organizing map (SOM) is a data-driven method which requires no preliminary knowledge developed by (Kohonen, 1998). It is an unsupervised artificial neural network model that was widely applied in complex data analysis without preliminary knowledge. The mechanism of SOM resembles the process of human brains that it can self-organize neurons with the same weight vector as the input vectors, and cluster the spatial distribution of similar-function neurons (Wang et al., 2020a, b, c, d). The ordered neurons were connected through a neighborhood relation on a SOM map. Similar color gradients represent positive correlations and antiparallel color gradients show negative correlations. Two error parameters, including quantization error (QE) and topological error (TE), were used to control the SOM modeling quality. Firstly, the number of input samples (N) was 130, which showed 130 soil samples collected in the study area. Secondary, the number of neurons (M) was calculated by the formula as follows: $M = 5\sqrt{N} \approx 55$ according to the empirical equation. Finally, the final number of neurons (M) in the neural matrix was composited of 7*8 neurons by considering QE and TE. SOM Toolbox in MATLAB was utilized to apportion the sources of soil heavy metals.

Results and discussion

Descriptive analysis of heavy metal concentrations in Hulan River Watershed

The descriptive analysis of the soil heavy metal concentrations is shown in Table 1. The concentration ranges of heavy metals of As, Hg, Cr, Ni, Cu, Zn, Cd, and Pb were 3.52–27.97, 0.01–0.21, 16.12–78.12, 6.99–249.98, 5.64–940.28, 21.6–314.28, 0.04–1.21, and 15.77–38.5 mg/kg, with corresponding mean values of 10.00, 0.03, 51.91, 26.76, 27.71, 68.39, 0.15, and 24.64 mg/kg, and median values of 9.66,

Table 1 Descriptive statistics of soil heavy metals in the study area (mg/kg)

	As	Hg	Cr	Ni	Cu	Zn	Cd	Pb
Min	3.52	0.01	16.12	6.99	5.64	21.60	0.04	15.77
Max	27.97	0.21	78.12	249.98	940.28	314.28	1.21	38.50
Mean	10.00	0.03	51.91	26.76	27.71	68.39	0.15	24.64
Median	9.66	0.03	54.30	25.99	20.61	64.65	0.13	24.68
Standard deviation	2.83	0.02	9.87	20.30	80.86	28.89	0.11	2.99
Coefficient variation	28.25%	73.48%	19.02%	75.86%	291.79%	42.25%	76.08%	12.13%
Skewness	3.38	4.82	−1.39	10.43	11.32	5.38	7.02	0.50
Kurtosis	19.38	30.48	3.30	115.62	128.67	41.42	62.54	3.57
Risk screening value	30.00	2.40	200.00	100.00	100.00	250.00	0.30	120.00
Background value	9.14	0.03	42.46	23.65	17.78	52.05	0.07	20.23
Higher than background value (%)	74.01%	80.77%	53.85%	73.85%	73.85%	81.54%	88.46%	87.69%
Higher than risk screening value (%)	0.00%	0.00%	0.00%	0.77%	0.77%	0.77%	3.08%	0.00%

0.03, 54.3, 25.99, 20.61, 64.65, 0.13, and 24.68 mg/kg, respectively. Approximately all the heavy metals of the soil samples exceeded the corresponding background value of the soil in Heilongjiang province (Sun et al., 2013). In addition, there were 0.77% and 3.08% of sampling locations showing higher concentration values than the risk screening values for Ni/Cu/Zn and Cd, respectively. According to the Costa's classification (Costa et al., 2019) (high variation: CV > 35%, medium variation: 16 < CV ≤ 35%, low variation: CV ≤ 16%), Cd, Ni, Hg, Cu, and Zn in the study area showed high variations, implying the anthropogenic activities such as industrial emission, traffic emission, and fertilizers might be the important sources for these heavy metals. As and Cr showed median variations, suggesting they might be affected by both anthropogenic activities and natural factors.

Evaluation of soil heavy metal pollution

Pollution evaluation of soil heavy metals

The summary of PLI and PI is shown in Table 2. The mean PI values of As, Hg, Cr, Ni, Cu, Zn, Cd, and Pb were 1.16, 1.56, 0.97, 1.15, 1.49, 1.22, 1.64, and 1.14,

respectively, suggesting all the heavy metals except Cr in this area were slightly polluted. The percentages of soil samples showing PI values larger than 1 for As, Hg, Cr, Ni, Cu, Zn, Cd, and Pb were 74.01%, 80.77%, 53.85%, 73.85%, 73.85%, 81.54%, 88.46%, 87.69%, and 81.54%, respectively, suggesting most of the soil sampling sites were heavy metal polluted. According to the classification of PLI, 83.08% of the soil samples were slightly or mildly polluted, and 1.54% of the soil samples were severely polluted, and only 16.92% of the soil samples were unpolluted.

Ecological evaluation of soil heavy metals

The order of mean EI values of the heavy metals in soil samples was Hg (62.30) > Cd (49.22) > As (11.63) > Cu (7.45) > Pb (5.68) > Ni (5.74) > Cr (1.94) > Zn (1.22) (Table 3). All soils experienced low ecological risk with all the heavy metals except Hg and Cd. As the toxic-response factor of Hg and Cd is higher than other soil heavy metals, EI mean values of Hg and Cd were larger than 40, showing both heavy metals reached moderate risk level. A total of 80.77% and 60.77% of the soil samples exceeded the low risk level for Hg and Cd,

Table 2 Summary statistics of the Single factor Pollution Index (PI) and Pollution Load Index (PLI) in the agricultural soils of Hulan River Watershed

	As	Hg	Cr	Ni	Cu	Zn	Cd	Pb	PLI
Mean	1.16	1.56	0.97	1.15	1.49	1.22	1.64	1.14	1.19
Min	0.41	0.45	0.30	0.30	0.30	0.39	0.47	0.73	0.41
Max	3.25	10.29	1.46	10.73	50.55	5.62	13.41	1.77	3.58
Pollution %	74.01%	80.77%	53.85%	73.85%	73.85%	81.54%	88.46%	87.69%	83.08%

Table 3 Summary statistics of Ecological risk index (EI) and Comprehensive ecological risk assessment (RI) in the agricultural soils of Hulan River Basin

	As	Hg	Cr	Ni	Cu	Zn	Cd	Pb	RI
Mean	11.63	62.30	1.94	5.74	7.45	1.22	49.22	5.68	145.19
Min	4.09	17.80	0.60	1.50	1.52	0.39	14.00	3.63	45.63
Max	32.52	411.60	2.91	53.64	252.76	5.62	402.33	8.87	553.15
Beyond low risk %	0.00%	80.77%	0.00%	0.77%	0.77%	0.00%	60.77%	0.00%	24.62%

respectively. RI combined ecological risk from all heavy metals and they ranged from 45.63 to 553.15 with the mean value of 145.19, indicating low combined ecological risk of soil heavy metals across the Hulan River Watershed. Only 24.62% of the soil samples exceeded the low risk level of RI (Table 3).

Health risk evaluation of soil heavy metals

The average HI values were all below 1 for adult and children, and the average THI and TCR values were

Table 4 Mean value of non-carcinogenic risk index and carcinogenic risk index of soil heavy metals based on three exposure pathways

|	Male	Female	Children
Non-carcinogenic risk index			
HI-As	1.42E−01	1.65E−01	7.00E−01
HI-Hg	1.49E−04	1.74E−04	4.81E−03
HI-Cr	5.83E−02	6.80E−02	3.19E−01
HI-Ni	2.12E−03	2.47E−03	1.77E−02
HI-Cu	1.06E−03	1.23E−03	9.00E−03
HI-Zn	3.64E−04	4.23E−04	3.00E−03
HI-Cd	7.86E−04	9.16E−04	3.57E−03
HI-Pb	1.17E−02	1.36E−02	9.41E−02
$THI_{Ingestion}$	8.42E−02	9.81E−02	7.62E−01
$THI_{Inhalation}$	3.63E−04	4.22E−04	1.63E−03
THI_{Dermal}	1.32E−01	1.54E−01	3.87E−01
THI	2.17E−01	2.52E−01	1.15E+00
Carcinogenic risk index			
CR-As	2.19E−05	2.55E−05	2.70E−05
CR-Cr	1.26E−05	1.47E−05	2.82E−05
CR-Ni	2.18E−05	2.54E−05	4.91E−05
CR-Cd	5.44E−11	6.33E−11	6.12E−11
$TCR_{Ingestion}$	4.15E−05	4.83E−05	9.34E−05
$TCR_{Inhalation}$	1.38E−07	1.60E−07	1.55E−07
TCR_{Dermal}	1.47E−05	1.71E−05	1.08E−05
TCR	5.63E−05	6.56E−05	1.04E−04

also higher than 1 and 1E−04 for children, respectively (Table 4). The results suggest the non-carcinogenic and carcinogenic risks of the soil heavy metals in the study area were not in an acceptable range for the children. The values of three exposure pathways for average THI and TCR were in the order of $THI_{der} > THI_{ing} > THI_{inh}$, and $TCR_{ing} > TCR_{der} > TCR_{inh}$, respectively, suggesting ingestion and derma contact were two major pathways for heavy metal health risks. For As, Cr, and Ni, the average HI accounted for THI was in the order of As (62.21%) > Cr (27.47%) > Ni (1.37%), and the average CR accounted for TCR was in the order of Ni (42.60%) > As (32.92%) > Cr (24.49%). The non-carcinogenic and carcinogenic risk indices for children were higher than those for adult males and females, which is confirmed by other research (Amin et al., 2013; Li et al., 2021).

Source analysis of soil heavy metals based on PMF and SOM

Figure 2 shows the contributions of sources of soil heavy metals. Factor 1 was dominated by Hg with the loadings of 99.8%. Factor 1 was also moderately loaded with Cd (34.7%), As (21.0%), and Pb (21.0%) (Fig. 2). The high concentration of Hg was shown in the central part of the study area where coal steam-electric plant is built (Fig. 4). Multiple research also indicated that coal burning and atmospheric deposition were the major sources of Hg (Cooke et al., 2020; Liu et al., 2021a, b). Some research proved Cd, As, and Pb were important elements imported into the soil during atmospheric deposition (Luo et al., 2009; Zhao et al., 2019). As a result, factor 1 is considered as industrial emission and atmospheric deposition.

Factor 2 was moderately loaded by Pb (33.6%) and Cd (24.6%). Previous studies showed that Pb in soil was regarded as one of the contaminants of traffic emission. Pb can not only be released from vehicle

Fig. 2 Profiles and contributions of sources of soil heavy metals from PMF model
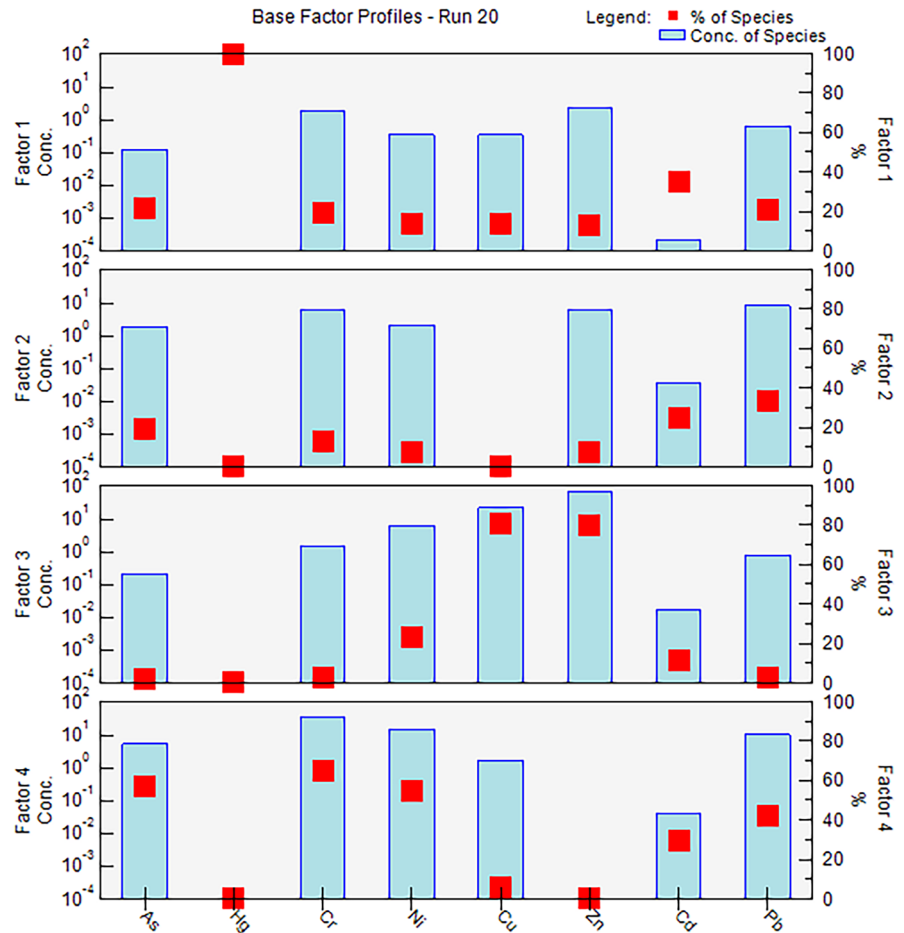
tires and brake pad (Xiao et al., 2020), but also from road dust deposit (Yesilkanat & Kobya, 2021). The area close to the major highways and roads in the study area had relative higher Pb concentration compared with other areas (Fig. 3). Some research proved that traffic was an important source of Cd (Jayarathne et al., 2018). Therefore, factor 2 is considered as traffic emission.

Factor 3 was highly dominated by Cu and Zn with the loadings of 80.6% and 80.0% (Fig. 2). Previous studies have shown that farming practices, such as the application of fertilizer, pesticide, and livestock manure, were perceived to be the predominant sources of Cu and Zn (Manoj & Kawsar, 2020; Shen et al., 2020). Relatively high concentration of Cu was shown in the northern part of the study area where the major land use type is upland planted with maize. In addition, high concentration of Zn was overlapped

with the spatial distribution of livestock farms, suggesting the livestock manure and effluent discharge from the livestock farms may lead to the Zn pollution in those areas. As a result, factor 3 is considered as agricultural source.

Factor 4 was described by Cr, As, Ni, Pb, and Cd concentration with the loadings of 65.3%, 56.7%, 54.7%, 42.3%, and 29.2%. Therefore, Cr, As, Ni, and Pb were the principal elements to demonstrate the source of pollution in factor 4. It is well known that those heavy metals could stem from mixed sources including natural source, sewage irrigation, industrial activities, and other anthropogenic origins (Chai et al., 2021; Heidari et al., 2021). Relatively high Cr concentration was shown in the central part of the study area where urban area of Hulan District is located. Multiple factories, residential areas, roads, and commercial buildings could be the important

Fig. 3 SOM map of concentration of soil heavy metals
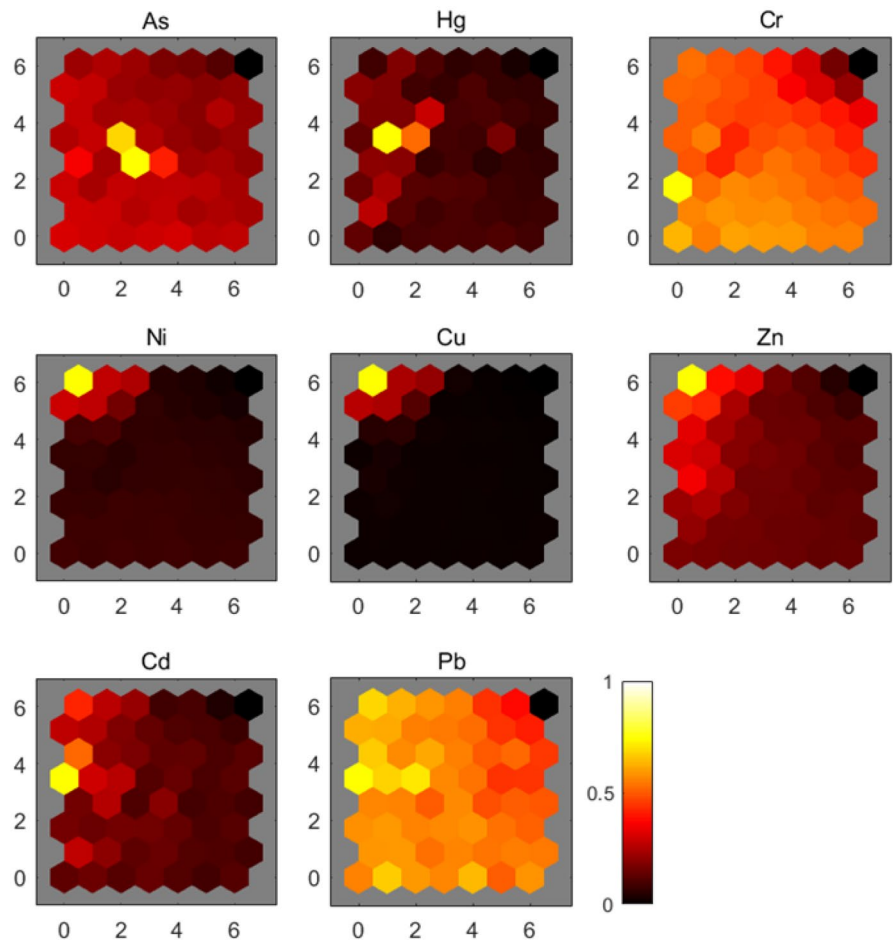
anthropogenic sources of Cr in the central part of the study area. The farmland in the northeastern part of the study area and Hulan River estuary area also had relatively high As concentration. Various research already had proved that fertilizer, pesticide, and manure were the major sources of Cr, As, and Ni in agricultural area (Kharazi et al., 2021; Setia et al., 2021). As a result, factor 4 is poised to be a combination of agricultural source, natural source, industrial emission, traffic emission, and atmospheric deposition.

Figure 3 is the SOM diagram of soil heavy metal concentration in the study area. The image shows the weight of each soil heavy metal of the input vector. The lighter the color, the greater the weight. If two soil heavy metals are similar in color on a component plane, it indicates that the two soil heavy metals are positively correlated and have a common source. It can be seen from Fig. 3 that the color gradients of Cr

and Pb are similar, indicating that Cr and Pb are positively correlated and may have a common source of pollution, which is confirmed by PMF analysis as a mixed source. The color gradients of Zn and Cu are comparable and highly distributed at the upper left corner, which are very different from those of Cr and Pb. The left neurons of the maps show overall high concentration of Hg and Cd compared with right neurons of the maps.

Spatial analysis of soil heavy metals

*Spatial pattern of soil heavy metal concentrations*

Spatial pattern of all the heavy metals is shown in Fig. 4. Multiple research already concluded that anthropogenic activities such as fertilizers, pesticides, herbicides, and sewage irrigation can contribute to the enrichment of Cr and Pb in agricultural

soil (Kharazi et al., 2021; Liu et al., 2021a, b). Relatively high Cr concentration was shown in the eastern part of the study area where the coal steam-electric plants, plastic steel factories, pharmaceutical factories, building materials factories, residential areas, commercial buildings, and roads could be the major anthropogenic sources of Cr. Relatively higher Pb concentration was displayed in the areas close to the major highways and roads. The spatial distributions of Ni and Cu were similar. Some farmlands in the northern part of the study area showed remarkable higher Ni and Cu concentration compared with other areas. It is highly possible that farmlands in this area experienced accumulation due to the agricultural activities such as fertilizer, pesticide, and sewage irrigation. High Zn concentration displayed spotty pattern across the study area. Hot spots of As emerged in the northeastern part of the Hulan River Watershed where there are multiple food processing plants located in Baikui town and Huangjia town in Hulan District (Fig. 4f). High Hg concentration was mainly distributed in the central part of the study area, which is overlapped with the spatial distribution of the coal steam-electric plants

(Fig. 4g). Relatively high Cd concentration was shown in the Hulan Estuary. The increasing discharge of industrial and domestic effluents from the Hulan River may contribute to the accumulation of Cd in the study area. Multiple research also found the accumulation of Cd appears in other river estuaries such as Yangtze River Estuary of China (Wang et al., 2021), Scheldt estuary of Europe (Gaulier et al., 2021), and Mlalazi estuary of South Africa (Adeleke et al., 2020).

Spatial pattern of the source contributions to the soil heavy metals

The factor scores were plotted using IDW method (Fig. 5). Factor 1 (atmospheric deposition and industrial emission) was highly concentrated in the central part of the study area where coal steam-electric plants discharged heavy metals such as Hg. Factor 1 was also highly loaded in the southeastern part of the study area where urban areas had high contribution of the atmospheric deposition and industrial emission. Factor 2 (traffic source) was widely distributed in the western and southern part of the study area where
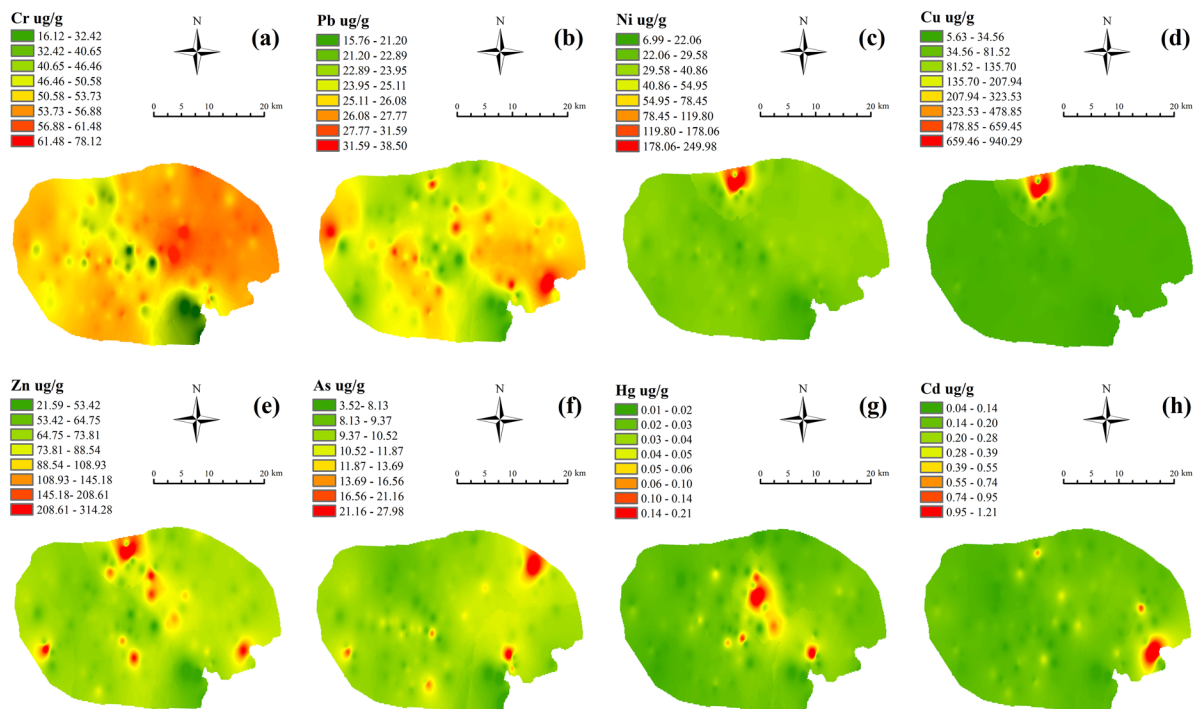
Fig. 4 Spatial distribution maps of soil (**a**) Cr, (**b**) Pb, (**c**) Ni, (**d**) Cu, (**e**) Zn, (**f**) As, (**g**) Hg, and (**h**) Cd

Fig. 5 (a-d) The spatial distribution of source contribution to soil heavy metals in the study area
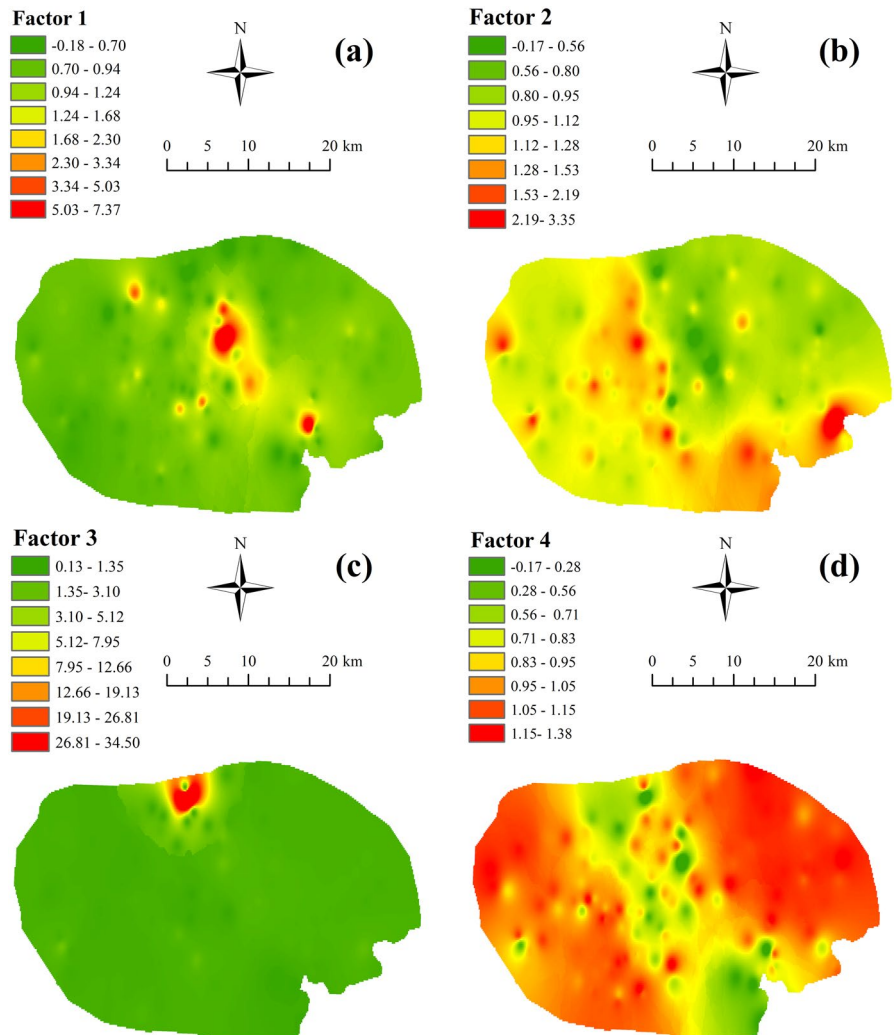

multiple expressways and highways were built. Factor 3 (agricultural source) was highly loaded in a small farmland area located in the northern part of the study area where farmlands in this area had significantly higher Ni, Cu, and Zn concentration compared with other areas. Factor 4 was widely distributed in the study area as it was a combination of agricultural source, industrial emission, atmospheric deposition, and natural source.

Spatial pattern of the pollution, ecological risk and health risk indices of soil heavy metals

Figure 6 shows the spatial pattern of PI and PLI of heavy metals in the study area. According to Fig. 6,

most of study area was unpolluted and slightly polluted for As, Cr, Cu, Ni, Pb, and Zn. Hulan Estuary area was highly polluted by Cd, and some farmlands in the study area were also mildly or moderately polluted by Cd. Most of the study area was moderately contaminated by soil heavy metals according to the spatial pattern of the PLI (Fig. 6i).

Figure 7 shows the spatial pattern of ecological risk indices of soil heavy metals in the study area. As, Cu, Cr, Ni, Pb, and Zn posed low ecological risk in most of the study area. Considerable and high ecological risk from Hg existed in the central part of the study area, and considerable and high ecological risk from Cd existed in the Hulan River estuary. RI values in the eastern part of the study
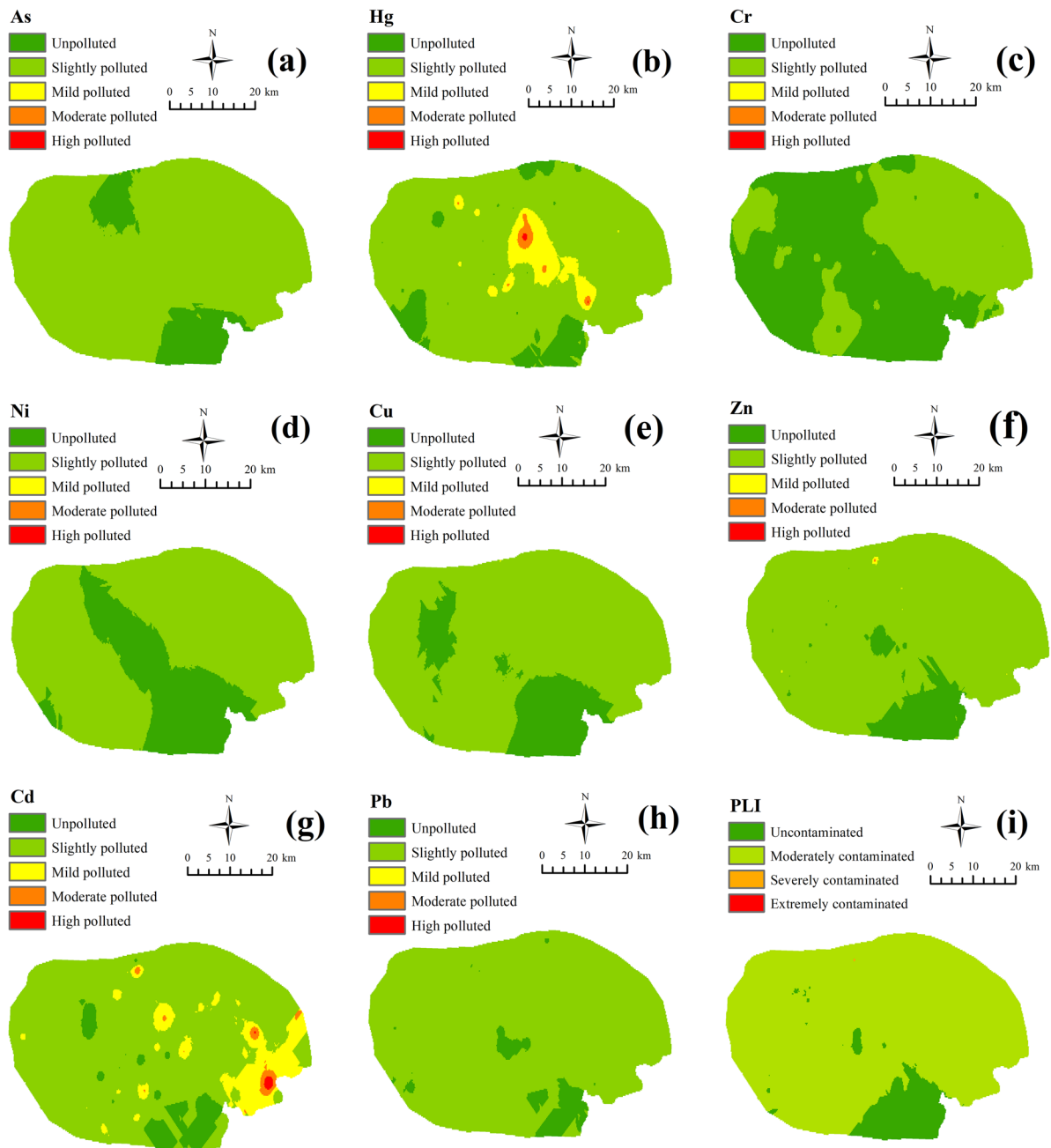
Fig. 6 Spatial distributions of pollution index (*PI*) (**a-h**) and pollution load index (PLI) (**i**) for heavy metals in Hulan River Basin

area were higher compared with the western part of the study area (Fig. 7). In general, the spatial pattern of RI revealed that the eastern part of the study area experienced moderate ecological risk of soil heavy metals.

The average THI ranged between 0.08 and 0.47 for adult males, 0.09–0.55 for adult females, and 0.44–2.38 for children (Fig. 8a–c). From Fig. 8c, the average THI for children in most of the study area exceeded 1, suggesting that children experienced non-carcinogenic risk
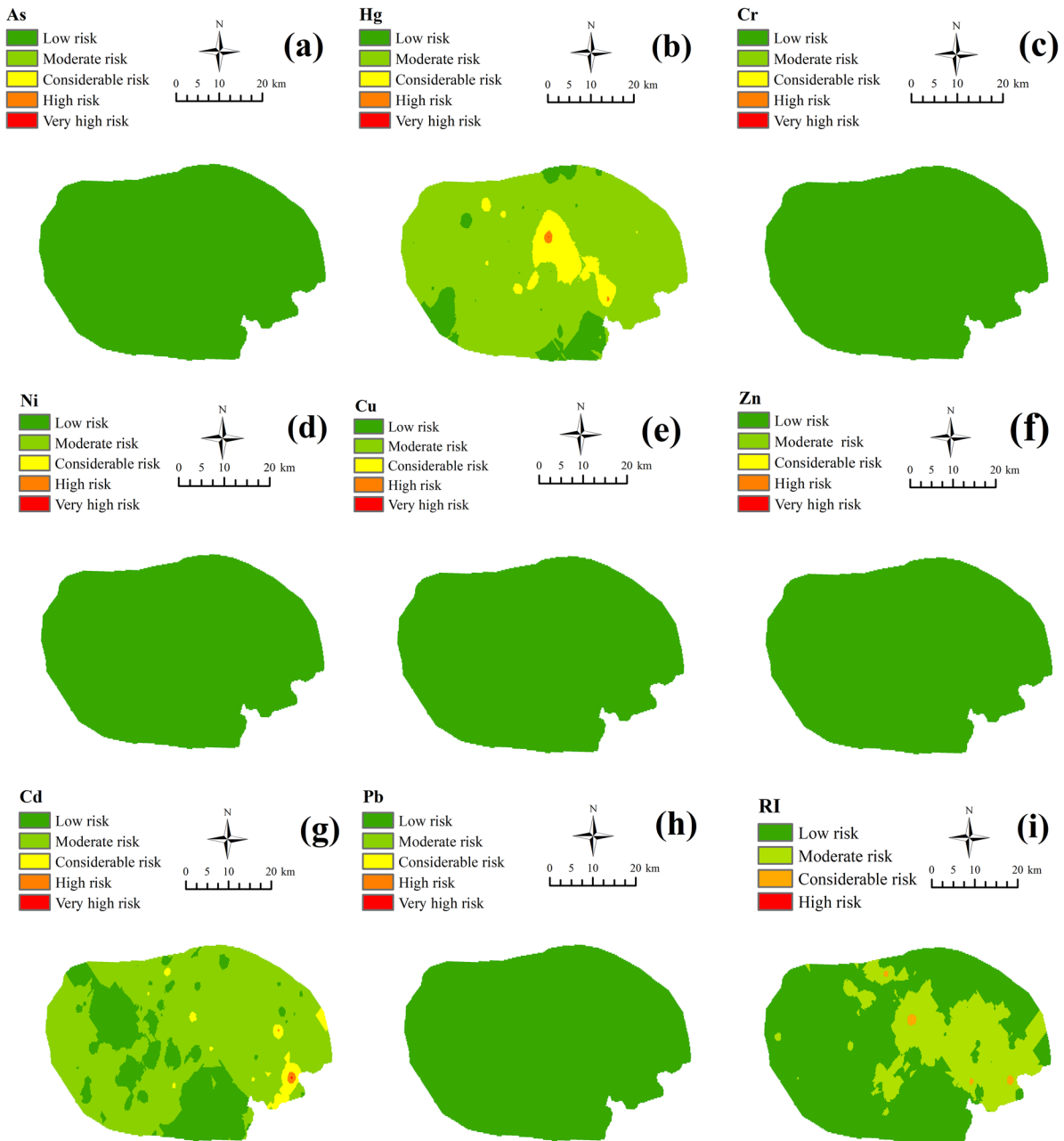
Fig. 7 Spatial distributions of pollution ecological risk indices (EI) (**a-h**) and integrated ecological risk index (RI) (**i**) for heavy metals in Hulan River Basin

in most of the study area. From Fig. 8d–f, the average TCR ranged between $1.81E-05$ and $2.34E-04$ for adult male, and $2.11E-05$–$2.72E-04$ for adult male, and $3.22E-05$–$5.06E-04$ for children. The average TCR for adult males and females in a small area located in the northern part of the study area exceeded

$1.0E-04$, suggesting adults in this area experienced carcinogenic risks. The spatial pattern of TCR for children also revealed that most of the study area showed relatively high TCR ($>1.0E-04$), suggesting children in these areas also experienced carcinogenic risks. In general, the non-carcinogenic and carcinogenic risks
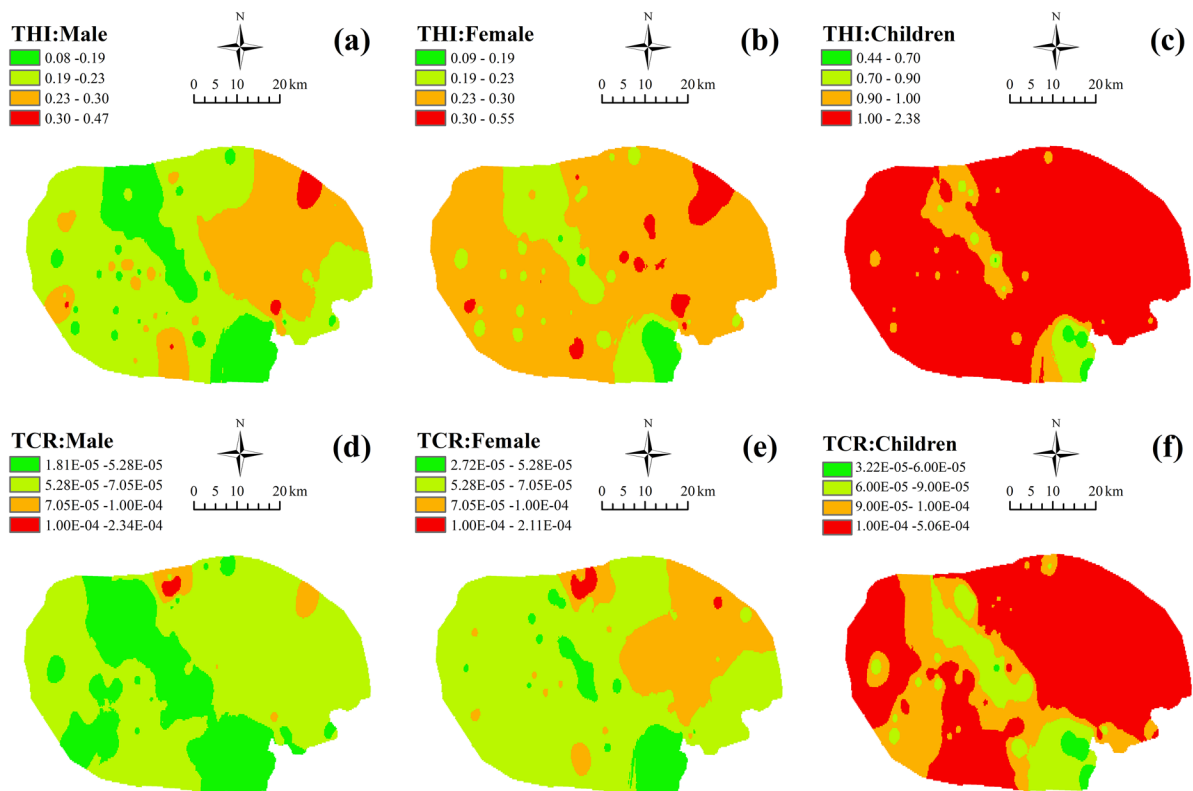
Fig. 8 (a-f) Spatial distributions of health risks for heavy metals in Hulan River Basin

for adult and children along the Hulan River were lower than other areas, and children in most of the study area experienced carcinogenic and non-carcinogenic risks.

In general, considerable and high ecological risk from Hg existed in the area close to the coal steam-electric plant, and considerable and high ecological risk from Cd existed in the Hulan River estuary area. Children in most of the Hulan River Watershed experienced carcinogenic and non-carcinogenic risks. Zonal pollution control and soil restoration measures should be implemented in the areas with high ecological and health risks.

Comparison with other soil heavy metal studies

Compared with other Northeastern China cities (Table S4), the mean concentration of Cu in this study area was the highest. In this area, the mean As concentration is higher than Changchun and Baicheng-songyuan Area, and the mean concentration of Ni showed lower concentration compared with Shenyang. Mean Cr concentration is higher than Changchun, Dehui, and Baichang-Songyuan area. Compared with the research conducted in Eastern China, the average concentration of Cd, Hg, Pb, and Zn was lower than those research in Eastern China. In North China, As and Cd of Tianjin and Shanxi were higher than Hulan River Watershed. The concentrations of all the soil heavy metals in the study areas of Central China were higher than those in Hulan River Watershed. Compared with the study areas in South China, the concentrations of all the soil heavy metals except Hg and Pb in Hulan River Watershed were higher than those in Guandong, while the concentrations of all the soil heavy metals except As in Hulan River Watershed were higher than those in Sanya. The concentrations of all the soil heavy metals in Hulan River Watershed were lower compared with other study areas in other developing countries such as India and Nigeria.

Conclusion

The concentrations of all the heavy metals in the soil samples exceeded the background values in the study area. The mean PI value of As, Hg, Cr, Ni, Cu, Zn, Cd, and Pb was 1.16, 1.56, 0.97, 1.15, 1.49, 1.22, 1.64, and 1.14, respectively, suggesting all the heavy metals except Cr in this area were slightly polluted. According to PLI, 83.08% of the soil samples were slightly or mildly polluted, and 1.54% of the soil samples were severely polluted, and only 16.92% of the soil samples were unpolluted. All soils belonged to the low ecological risk categories except Cd and Hg based on EI values. In addition, non-carcinogenic and carcinogenic risks for the children owed to the soil heavy metals were not in an acceptable range. Based on the PMF and SOM analysis, four potential sources were revealed including (1) atmospheric deposition and industrial emission; (2) traffic source; (3) agricultural source; and (4) a combination of agricultural source, industrial emission, traffic emission, and natural source. Considerable and high ecological risk from Hg existed in the area close to the coal steam-electric plant, and considerable and high ecological risk from Cd existed in the Hulan River estuary area. The eastern part of the study area experienced higher non-carcinogenic and carcinogenic risks for adults and children than the western part of the study area. Zonal pollution control and soil restoration measures should be taken in the areas with high ecological and health risks in Hulan River Watershed.

Declarations

Ethics approval and consent to participate Not applicable.

Consent for publication Not applicable.

Competing interests The authors declare no competing interests.

References

Adeleke, B., Robertson-Andersson, D., & Moodley, G. (2020). Comparative analysis of trace metal levels in the crab Dotilla fenestrata, sediments and water in Durban Bay harbour, Richards Bay harbour and Mlalazi estuary, Kwazulu-Natal, South Africa. *Heliyon, 6*(8), e04725. https://doi.org/10.1016/j.heliyon.2020.e04725

Amin, N.-, Hussain, A., Alamzeb, S., & Begum, S. (2013). Accumulation of heavy metals in edible parts of vegetables irrigated with waste water and their daily intake to adults and children, District Mardan, Pakistan. *Food Chemistry, 136*(3), 1515–1523. https://doi.org/10.1016/j.foodchem.2012.09.058

Bhuiyan, M. A. H., Karmaker, S. C., Bodrud-Doza, M., Rakib, M. A., & Saha, B. B. (2021). Enrichment, sources and ecological risk mapping of heavy metals in agricultural soils of Dhaka district employing SOM, PMF and GIS Methods. *Chemosphere, 263*, 128339. https://doi.org/10.1016/j.chemosphere.2020.128339

Brown, S. G., Eberly, S., Paatero, P., & Norris, G. A. (2015). Methods for estimating uncertainty in PMF solutions: Examples with ambient air and water quality data and guidance on reporting PMF results. *Science of the Total Environment, 518–519*, 626–635. https://doi.org/10.1016/j.scitotenv.2015.01.022

Buat-Menard, P., & Chesselet, R. (1979). Variable influence of the atmospheric flux on the trace metal chemistry of oceanic suspended matter. *Earth and Planetary Science Letters, 42*(3), 399–411. https://doi.org/10.1016/0012-821X(79)90049-9

Chai, L., Wang, Y., Wang, X., Ma, L., Cheng, Z., & Su, L. (2021). Pollution characteristics, spatial distributions, and source apportionment of heavy metals in cultivated soil in Lanzhou, China. *Ecological Indicators, 125*, 107507. https://doi.org/10.1016/j.ecolind.2021.107507

Christensen, E. R., Steinnes, E., & Eggen, O. A. (2018). Anthropogenic and geogenic mass input of trace elements to moss and natural surface soil in Norway. *Science of the Total Environment, 613–614*, 371–378. https://doi.org/10.1016/j.scitotenv.2017.09.094

Cooke, C. A., Martínez-Cortizas, A., Bindler, R., & Sexauer Gustin, M. (2020). Environmental archives of atmospheric Hg deposition – A review. *Science of the Total Environment, 709*, 134800. https://doi.org/10.1016/j.scitotenv.2019.134800

Costa, B. R. S., Oldoni, H., Silva, W. A., Martins, R. L., & Bassoi, L. H. (2019). Temporal variation and spatial distribution of relative indices of leaf chlorophyll in grapevine cv. chardonnay. *Engenharia Agrícola, 39*(spe), 74–84. https://doi.org/10.1590/1809-4430-eng.agric.v39nep74-84/2019

Dang, P., Gu, X., Lin, C., Xin, M., Zhang, H., Ouyang, W., et al. (2021). Distribution, sources, and ecological risks of

potentially toxic elements in the Laizhou Bay, Bohai Sea: Under the long-term impact of the Yellow River input. *Journal of Hazardous Materials, 413*, 125429. https://doi.org/10.1016/j.jhazmat.2021.125429

Fei, X., Xiao, R., Christakos, G., Langousis, A., Ren, Z., Tian, Y., & Lv, X. (2019). Comprehensive assessment and source apportionment of heavy metals in Shanghai agricultural soils with different fertility levels. *Ecological Indicators, 106*, 105508. https://doi.org/10.1016/j.ecolind.2019.105508

Gaulier, C., Zhou, C., Gao, Y., Guo, W., Reichstädter, M., Ma, T., et al. (2021). Investigation on trace metal speciation and distribution in the Scheldt estuary. *Science of the Total Environment, 757*, 143827. https://doi.org/10.1016/j.scitotenv.2020.143827

Gujre, N., Mitra, S., Soni, A., Agnihotri, R., Rangan, L., Rene, E. R., & Sharma, M. P. (2021). Speciation, contamination, ecological and human health risks assessment of heavy metals in soils dumped with municipal solid wastes. *Chemosphere, 262*, 128013. https://doi.org/10.1016/j.chemosphere.2020.128013

Hakanson, L. (1980). An ecological risk index for aquatic pollution control.a sedimentological approach. *Water research, 14*(8), 975–1001. https://doi.org/10.1016/0043-1354(80)90143-8

Heidari, M., Darijani, T., & Alipour, V. (2021). Heavy metal pollution of road dust in a city and its highly polluted suburb; quantitative source apportionment and source-specific ecological and health risk assessment. *Chemosphere, 273*, 129656. https://doi.org/10.1016/j.chemosphere.2021.129656

Hou, D., O'Connor, D., Igalavithana, A. D., Alessi, D. S., Luo, J., Tsang, D. C. W., et al. (2020). Metal contamination and bioremediation of agricultural soils for food safety and sustainability. *Nature Reviews Earth & Environment, 1*(7), 366–381. https://doi.org/10.1038/s43017-020-0061-y

Ikem, A., Egiebor, N. O., & Nyavor, K. (2003). Trace elements in water, fish and sediment from Tuskegee Lake, Southeastern USA. *Water, Air, and Soil Pollution, 149*(1), 51–75. https://doi.org/10.1023/A:1025694315763

Jayarathne, A., Egodawatta, P., Ayoko, G. A., & Goonetilleke, A. (2018). Role of residence time on the transformation of Zn, Cu, Pb and Cd attached to road dust in different land uses. *Ecotoxicology and Environmental Safety, 153*, 195–203. https://doi.org/10.1016/j.ecoenv.2018.02.007

Jiang, H.-H., Cai, L.-M., Hu, G.-C., Wen, H.-H., Luo, J., Xu, H.-Q., & Chen, L.-G. (2021). An integrated exploration on health risk assessment quantification of potentially hazardous elements in soils from the perspective of sources. *Ecotoxicology and Environmental Safety, 208*, 111489. https://doi.org/10.1016/j.ecoenv.2020.111489

Karaouzas, I., Kapetanaki, N., Mentzafou, A., Kanellopoulos, T. D., & Skoulikidis, N. (2021). Heavy metal contamination status in Greek surface waters: A review with application and evaluation of pollution indices. *Chemosphere, 263*, 128192. https://doi.org/10.1016/j.chemosphere.2020.128192

Kharazi, A., Leili, M., Khazaei, M., Alikhani, M. Y., & Shokoohi, R. (2021). Human health risk assessment of heavy metals in agricultural soil and food crops in Hamadan, Iran. *Journal of Food Composition and Analysis, 100*, 103890. https://doi.org/10.1016/j.jfca.2021.103890

Kohonen, T. (1998). The self-organizing map. *Neurocomputing, 21*(1), 1–6. https://doi.org/10.1016/S0925-2312(98)00030-7

Li, L., Zhang, Y., Ippolito, J. A., Xing, W., & Tu, C. (2021). Lead smelting alters wheat flour heavy metal concentrations and health risks. *Journal of Environmental Quality, 50*(2), 454–464. https://doi.org/10.1002/jeq2.20198

Liu, H., Zhang, Y., Yang, J., Wang, H., Li, Y., Shi, Y., et al. (2021a). Quantitative source apportionment, risk assessment and distribution of heavy metals in agricultural soils from southern Shandong Peninsula of China. *Science of the Total Environment, 767*, 144879. https://doi.org/10.1016/j.scitotenv.2020.144879

Liu, S., Wang, X., Guo, G., & Yan, Z. (2021b). Status and environmental management of soil mercury pollution in China: A review. *Journal of Environmental Management, 277*, 111442. https://doi.org/10.1016/j.jenvman.2020.111442

Luo, L., Ma, Y., Zhang, S., Wei, D., & Zhu, Y.-G. (2009). An inventory of trace element inputs to agricultural soils in China. *Journal of Environmental Management, 90*(8), 2524–2530. https://doi.org/10.1016/j.jenvman.2009.01.011

Lv, J. (2019). Multivariate receptor models and robust geostatistics to estimate source apportionment of heavy metals in soils. *Environmental Pollution, 244*, 72–83. https://doi.org/10.1016/j.envpol.2018.09.147

Manoj, M. C., & Kawsar, M. (2020). Metal contamination assessment in a sediment core from Vagamon Lake, southwest India: Natural/anthropogenic impact. *Environmental Nanotechnology, Monitoring & Management, 14*, 100362. https://doi.org/10.1016/j.enmm.2020.100362

Mao, D., He, X., Wang, Z., Tian, Y., Xiang, H., Yu, H., et al. (2019). Diverse policies leading to contrasting impacts on land cover and ecosystem services in Northeast China. *Journal of Cleaner Production, 240*, 117961. https://doi.org/10.1016/j.jclepro.2019.117961

Muller, G. (1969). Index of geoaccumulation in sediments of the Rhine River. *GeoJournal, 2*(3), 109–118.

Paatero, P., & Tapper, U. (1994). Positive matrix factorization: A non-negative factor model with optimal utilization of error estimates of data values. *Environmetrics, 5*(2), 111–126. https://doi.org/10.1002/env.3170050203

Pandey, B., Agrawal, M., & Singh, S. (2014). Assessment of air pollution around coal mining area: Emphasizing on spatial distributions, seasonal variations and heavy metals, using cluster and principal component analysis. *Atmospheric Pollution Research, 5*(1), 79–86. https://doi.org/10.5094/APR.2014.010

Semenkov, I., & Koroleva, T. (2020). Heavy metals content in soils of Western Siberia in relation to international soil quality standards. *Geoderma Regional, 21*, e00283. https://doi.org/10.1016/j.geodrs.2020.e00283

Sergeev, A. P., Buevich, A. G., Baglaeva, E. M., & Shichkin, A. V. (2019). Combining spatial autocorrelation with machine learning increases prediction accuracy of soil heavy metals. *CATENA, 174*, 425–435. https://doi.org/10.1016/j.catena.2018.11.037

Setia, R., Dhaliwal, S. S., Singh, R., Kumar, V., Taneja, S., Kukal, S. S., & Pateriya, B. (2021). Phytoavailability and human risk assessment of heavy metals in soils and food

crops around Sutlej river, India. *Chemosphere, 263*, 128321. https://doi.org/10.1016/j.chemosphere.2020.128321

Shen, X., Zeng, J., Zhang, D., Wang, F., Li, Y., & Yi, W. (2020). Effect of pyrolysis temperature on characteristics, chemical speciation and environmental risk of Cr, Mn, Cu, and Zn in biochars derived from pig manure. *Science of the Total Environment, 704*, 135283. https://doi.org/10.1016/j.scitotenv.2019.135283

Shi, T., Ma, J., Wu, F., Ju, T., Gong, Y., Zhang, Y., et al. (2019). Mass balance-based inventory of heavy metals inputs to and outputs from agricultural soils in Zhejiang province, China. *Science of the Total Environment, 649*, 1269–1280. https://doi.org/10.1016/j.scitotenv.2018.08.414

Song, X.-D., Yang, F., Ju, B., Li, D.-C., Zhao, Y.-G., Yang, J.-L., & Zhang, G.-L. (2018). The influence of the conversion of grassland to cropland on changes in soil organic carbon and total nitrogen stocks in the Songnen Plain of Northeast China. *CATENA, 171*, 588–601. https://doi.org/10.1016/j.catena.2018.07.045

Sun, G., Chen, Y., Bi, X., Yang, W., Chen, X., Zhang, B., & Cui, Y. (2013). Geochemical assessment of agricultural soil: A case study in Songnen-Plain (Northeastern China). *CATENA, 111*, 56–63. https://doi.org/10.1016/j.catena.2013.06.026

Wan, D., Song, L., Yang, J., Jin, Z., Zhan, C., Mao, X., et al. (2016). Increasing heavy metals in the background atmosphere of central North China since the 1980s: Evidence from a 200-year lake sediment record. *Atmospheric Environment, 138*, 183–190. https://doi.org/10.1016/j.atmosenv.2016.05.015

Wang, F., Guan, Q., Tian, J., Lin, J., Yang, Y., Yang, L., & Pan, N. (2020a). Contamination characteristics, source apportionment, and health risk assessment of heavy metals in agricultural soil in the Hexi Corridor. *CATENA, 191*, 104573. https://doi.org/10.1016/j.catena.2020.104573

Wang, H., Yilihamu, Q., Yuan, M., Bai, H., Xu, H., & Wu, J. (2020b). Prediction models of soil heavy metal(loid)s concentration for agricultural land in Dongli: A comparison of regression and random forest. *Ecological Indicators, 119*, 106801. https://doi.org/10.1016/j.ecolind.2020.106801

Wang, S., Kalkhajeh, Y. K., Qin, Z., & Jiao, W. (2020c). Spatial distribution and assessment of the human health risks of heavy metals in a retired petrochemical industrial area, South China. *Environmental Research, 188*, 109661. https://doi.org/10.1016/j.envres.2020.109661

Wang, Z., Xiao, J., Wang, L., Liang, T., Guo, Q., Guan, Y., & Rinklebe, J. (2020d). Elucidating the differentiation of soil heavy metals under different land uses with geographically weighted regression and self-organizing map. *Environmental Pollution, 260*, 114065. https://doi.org/10.1016/j.envpol.2020.114065

Wang, Y., Liu, R., Miao, Y., Jiao, L., Cao, L., Li, L., & Wang, Q. (2021). Identification and uncertainty analysis of high-risk areas of heavy metals in sediments of the Yangtze River estuary, China. *Marine Pollution Bulletin, 164*, 112003. https://doi.org/10.1016/j.marpolbul.2021.112003

Wu, S., Zhou, S., Bao, H., Chen, D., Wang, C., Li, B., et al. (2019). Improving risk management by using the spatial interaction relationship of heavy metals and PAHs in urban soil. *Journal of Hazardous Materials, 364*, 108–116. https://doi.org/10.1016/j.jhazmat.2018.09.094

Wu, J., Li, J., Teng, Y., Chen, H., & Wang, Y. (2020a). A partition computing-based positive matrix factorization (PC-PMF) approach for the source apportionment of agricultural soil heavy metal contents and associated health risks. *Journal of Hazardous Materials, 388*, 121766. https://doi.org/10.1016/j.jhazmat.2019.121766

Wu, X., Chen, C., Vu, T. V., Liu, D., Baldo, C., Shen, X., et al. (2020b). Source apportionment of fine organic carbon (OC) using receptor modelling at a rural site of Beijing: Insight into seasonal and diurnal variation of source contributions. *Environmental Pollution, 266*, 115078. https://doi.org/10.1016/j.envpol.2020.115078

Xiao, X., Zhang, J., Wang, H., Han, X., Ma, J., Ma, Y., & Luan, H. (2020). Distribution and health risk assessment of potentially toxic elements in soils around coal industrial areas: A global meta-analysis. *Science of the Total Environment, 713*, 135292. https://doi.org/10.1016/j.scitotenv.2019.135292

Yang, Y., Yang, X., He, M., & Christakos, G. (2020). Beyond mere pollution source identification: Determination of land covers emitting soil heavy metals by combining PCA/APCS, GeoDetector and GIS Analysis. *CATENA, 185*, 104297. https://doi.org/10.1016/j.catena.2019.104297

Yesilkanat, C. M., & Kobya, Y. (2021). Spatial characteristics of ecological and health risks of toxic heavy metal pollution from road dust in the Black Sea coast of Turkey. *Geoderma Regional, 25*, e00388. https://doi.org/10.1016/j.geodrs.2021.e00388

Zang, F., Wang, S., Nan, Z., Ma, J., Zhang, Q., Chen, Y., & Li, Y. (2017). Accumulation, spatio-temporal distribution, and risk assessment of heavy metals in the soil-corn system around a polymetallic mining area from the Loess Plateau, northwest China. *Geoderma, 305*(Supplement C), 188–196. https://doi.org/10.1016/j.geoderma.2017.06.008

Zeng, Y., Bi, C., Jia, J., Deng, L., & Chen, Z. (2020). Impact of intensive land use on heavy metal concentrations and ecological risks in an urbanized river network of Shanghai. *Ecological Indicators, 116*, 106501. https://doi.org/10.1016/j.ecolind.2020.106501

Zhao, R., Guan, Q., Luo, H., Lin, J., Yang, L., Wang, F., et al. (2019). Fuzzy synthetic evaluation and health risk assessment quantification of heavy metals in Zhangye agricultural soil from the perspective of sources. *Science of the Total Environment, 697*, 134126. https://doi.org/10.1016/j.scitotenv.2019.134126